

Upper Bound Analysis for Forging of Trochoidal Gears

Jongung-Choi*, Hae-Yong Cho** and Chang-Yong Jo*

(Received June 2, 1998)

Forging of trochoidal gears has been investigated by means of upper-bound analysis. A kinematically admissible velocity field for forging of a trochoidal gear was proposed. A neutral surface has been used to represent the inward flow of material during forging operation by using a hollow billet with a flat punch. By using the suggested kinematically admissible velocity fields, the applied forces were successfully calculated and compared with experimental inspections. The experimental set-up was installed in a 200-ton hydraulic press for forging. The billets of Al 2218 aluminum alloys were slightly coated with phosphate. It was found that the theoretical solutions were useful to predict the forging load for forging of trochoidal gears.

Key Words :

Nomenclature

r, θ, z	: Cylindrical coordinate system
M	: Fillet radius, tooth radius[mm]
r_n	: Neutral surface radius[mm]
r_r	: Root circle radius[mm]
u	: Ram speed[mm/s]
$\dot{\epsilon}_i$: Effective strain rate for i zone
$\bar{\sigma}$: Flow stress
U_r, U_θ, U_z	: Velocity component for each direction
N	: Number of teeth
r_p	: Pitch circle radius[mm]
t	: Height of workpiece[mm]
α	: Half pitch angle[rad]
$ \Delta V $: Velocity discontinuity

1. Introduction

A significant and vital trend in the forging industry is toward increasing precision and reducing lead time. In the context of gear components, this is particularly critical. The forging operations

are carried out in a hard working condition such as high stress state. The prediction of load and pressure for forging is necessary to design a die that can be used in the hard working condition. By the above reasons, some analyzing methods have been developed. One of them is the upper bound method that can be applied to analyze the load and relative pressure of three-dimensional shaped component in plastic deformation. Some researchers have analyzed extrusion processes (Cho, 1991; Kim, 1996) and others have studied forging processes of various shaped components (Grover and Juneja, 1984; Ohga et al., 1985; Kondo et al., 1985; Abdul and Dean, 1986; Kiuchi, 1986; Kiuchi et al., 1989; Choi et al., 1994; Cho et al., 1995; Cho et al., 1996). Cho (1991) suggested the velocity field for extrusion of helical gear by using upper bound method and analyzed the stress distribution on the tooth of extrusion die during the operation. Kim (1996) suggested the velocity fields for square die extrusion of trochoidal gear by using UBET and compared the calculated results with experimental inspections. Juneja et al. (1984) and Kondo et al. (1985) analyzed forging of spur gear by upper bound method. To simplify the analysis, they assumed the tooth profile as a trapezoid. Abdul and Dean (1986) assumed the side of teeth as a straight line parallel to the center line of a tooth. Nevertheless,

* Korea Institute of Machinery & Methods, Changwon, Gyungnam, 641-010, Korea

** Dept. of Precision & Mechanical Engineering, Chungbuk National University, Gaesin-dong, Heungduk-ku, Cheongju, Chungbuk, 361-763, Korea

normal velocity is discontinuous on the shear surface in the analysis done by Juneja et al. (1984) and Kondo et al. (1985). The velocity field which Dean proposed could not be used to evaluate the boundary condition at the surface of the die. Kiuchi analyzed the forging of compounded components with square spline and non-axisymmetric parts using UBET. Choi et al. (1994) suggested upper bound solutions for forging of a spur gear whose tooth profile is assumed as a straight line. The circumferential velocity component is considered as zero in the tooth zone. So, the shear energy dissipation rate is the largest portion of the total energy. Cho et al. (1996) suggested the upper bound solution for involute spur gear with arc fillet by using a solid and a hollow billet and calculated the power requirements. Cho found that the final loads for forging of spur gear can be reduced by using the hollow billet with a larger inner radius. As mentioned above, there are several reports about forging of gear-like components. However, there is no report about forging of trochoidal gear by means of upper bound method.

In this study, a kinematically admissible velocity field for forging of trochoidal gear that was used in pump and timing belt pulley has been proposed to predict the final load. The power requirements were calculated by using the proposed velocity field and were compared with experimental inspections.

2. Upper Bound Analysis

The cylindrical coordinate system (r, θ, z) was used in this analysis. Throughout the analysis, following assumptions were employed.

- (1) The shape of free flow surface is a circle centered from gear center O .
- (2) The constant friction factor is considered on the interface of die/workpiece.
- (3) The diameter of billet is equal to that of root circle.
- (4) The workpiece is isotropic, homogeneous and rigid-work-hardening material.

The kinematically admissible velocity field should satisfy the volume constancy expressed as:

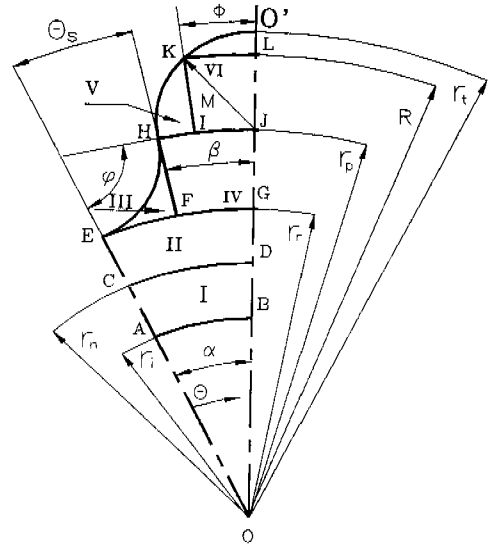


Fig. 1 Schematic drawing of half pitch for trochoidal gear.

$$\dot{\epsilon}_{rr} = \frac{\partial U_r}{\partial r}, \quad \dot{\epsilon}_{\theta\theta} = \frac{1}{r} \left(\frac{\partial U_\theta}{\partial \theta} + U_r \right), \quad \dot{\epsilon}_{zz} = \frac{\partial U_z}{\partial z},$$

$$\dot{\epsilon}_r = \dot{\epsilon}_{rr} + \dot{\epsilon}_{\theta\theta} + \dot{\epsilon}_{zz}$$

The boundary condition for the surface of workpiece is that the material should not flow across the die surface. To analyze forging of trochoidal gears, a generic deforming unit bounded two planes of symmetry with adjacent units as shown in Fig. 1. In practical use of pump, the tooth shape of trochoidal gear is either half-tooth high up to a fillet part or 2/3-tooth high up to a fillet part with some portion of the tooth circle. Material can neither cross nor shear along a plane of symmetry, hence it deforms within a unit which interacts, with adjacent units. The material is self-contained throughout the forging process. Each of the deforming units shown in Fig. 1. The unit is then further subdivided into six deformation zones labeled 1 ~ VI, where the plastic flow is assumed to take place.

If the punch moves down with unit velocity, the axial velocity U_z and the axial strain rate are given as follows:

$$U_z = -\frac{u}{t} z \quad (1)$$

where, t represents the current height of workpiece.

2.1 Kinematically admissible velocity field

2.1.1 For deformation zone I

$$(0 \leq \theta \leq \alpha, r_i \leq r \leq r_n)$$

This zone is assumed as an axisymmetric deformation zone. It is bounded by two planes of symmetry ($\theta = \alpha, \theta = 0$), neutral surface ($r = r_n$) and inner radius (r_i) as shown in Fig. 1. During the forging operation, material flows toward the gear center O with negative value. At the neutral surface, the radial velocity component should be zero. The velocity field for this zone is given as follows:

$$U_r = \frac{u}{2t} \left(r - \frac{r_n^2}{r} \right), U_\theta = 0$$

2.1.2 For deformation zone II

$$(0 \leq \theta \leq \alpha, r_n \leq r \leq r_p)$$

This zone is assumed as an axisymmetric deformation zone like the zone I. Although the appearances of velocity fields are the same with those of zone I, material of this zone flows toward the tooth zone with positive value.

$$U_r = \frac{u}{2t} \left(r - \frac{r_n^2}{r} \right), U_\theta = 0$$

2.1.3 For deformation zone III

$$(\beta \leq \theta \leq \alpha, r_r \leq r \leq r_p)$$

In this zone, the workpiece contacts the die surface EH, so the normal velocity with respect to the die wall is zero. The velocity field for this zone is given as follows:

$$U_r = \frac{u}{2t} \left(r - \frac{r_n^2}{r} \right), U_\theta = \frac{u}{2t} \left(r - \frac{r_n^2}{r} \right) \cot \varphi$$

$$\cot \varphi = \frac{(r_r + M)^4 - (r^2 - M^2) - (r^2 - r_r^2) [(2M + r_r)^2 - r^2]}{2(r_r + M)^2 \sqrt{(r^2 - r_n^2) [(2M + r_r)^2 - r^2]}}$$

2.1.4 For deformation zone IV

$$(0 \leq \theta \leq \beta, r_r \leq r \leq r_p)$$

In this zone, we represented the circumferential velocity as a linear function of angle θ . The velocity field for this zone is given as follows:

$$U_r = \frac{U_r}{2t} - \frac{C_1}{2t\beta r} + \frac{ur_n^2}{2t\beta} \frac{C_2}{r} + \frac{C_{IV}}{r}$$

$$U_\theta = \frac{u\theta}{2t\beta} \left[r - \frac{r_n^2}{r} \right] \cdot \cot \varphi$$

$$C_1 = \frac{1}{2} \sqrt{(r^2 - r_n^2) [(2M + r_r)^2 - r^2]} + 2r_n^2 \sin^{-1} \left[\frac{\sqrt{(2M + r_r)^2 - r^2}}{2\sqrt{M(r_r + M)}} \right]$$

$$C_2 = \frac{1}{2} (\tan^{-1} A + \tan^{-1} B) + \sin^{-1} \left[\frac{\sqrt{(2M + r_r)^2 - r^2}}{2\sqrt{M(r_r + M)}} \right] - \frac{1}{4(r_r + M)^2} \sqrt{(r^2 - r_n^2) [(2M + r_r)^2 - r^2]}$$

$$A = - \frac{(2M + r_r) \sqrt{(2M + r_r)^2 - r^2} + 4M(r_r + M)}{r_r(r^2 - r_n^2)}$$

$$B = - \frac{(2M + r_r) \sqrt{(2M + r_r)^2 - r^2} - 4M(r_r + M)}{r_r(r^2 - r_n^2)}$$

$$C_{IV} = \frac{\pi M^2}{2t\beta} - \frac{ur_n^2}{2t}$$

2.1.5 For deformation zone V

$$(\phi \leq \theta \leq \beta, r_p \leq r \leq R)$$

The workpiece contacts the die surface HK as shown in Fig. 1. The normal velocity with respect to the die surface should be zero. We assume that the circumferential velocity on the tooth profile is function of only radius r and the circumferential velocity in the deforming zone is a function of radius r . The velocity field for this zone is given as follows :

$$U_r = \frac{u \cdot r}{2t} + \frac{C_V}{r}$$

$$U_\theta = \left[\frac{u \cdot r}{2t} + \frac{C_V}{r} \right] \frac{r^2 - a \cdot b}{\sqrt{(a^2 - r^2)(r^2 - b^2)}}$$

Where, $a = r_p + M, b = r_p - M, C_V = \frac{u \cdot r_n^2}{2t\beta} C_2'' - \frac{u \cdot C_1''}{2t\beta} + C_{IV}, C_1'' = [C_1]_{r=r_p}, C_2'' = [C_2]_{r=r_p}$

2.1.6 For deformation zone VI

$$(0 \leq \theta \leq \phi, r_p \leq r \leq R)$$

We assume that the circumferential velocity is distributed as a linear function of angle. θ The velocity field for this zone is given as follows :

$$U_r = \frac{u \cdot r}{2t} + \frac{u}{2t} \frac{C_3}{\phi} + \frac{C_V}{r} \cdot \frac{C_4}{\phi} + \frac{C_{VI}}{r}$$

$$U_\theta = \frac{\theta}{\phi} \left[\frac{u \cdot r}{2t} + \frac{C_V}{r} \right] \frac{r^2 - a \cdot b}{\sqrt{(a^2 - r^2)(r^2 - b^2)}}$$

Where, $C_3 = \frac{\sqrt{(a^2 - r^2)(r^2 - b^2)} + (b - a)^2}{2}$

$$\sin^{-1} \sqrt{\frac{a^2 - r^2}{a^2 - b^2}}$$

$$C_4 = \sin^{-1} \sqrt{\frac{a^2 - r^2}{a^2 - b^2}} - \frac{1}{2} (\tan^{-1} C - \tan^{-1} D)$$

$$C = \frac{(b^2 - a^2 - a\sqrt{a^2 - r^2}) \cdot \sqrt{r^2 - b^2}}{b(b^2 - r^2)}$$

$$D = \frac{(b^2 - a^2 + a\sqrt{a^2 - r^2}) \cdot \sqrt{r^2 - b^2}}{b(b^2 - r^2)}$$

2.2 Energy dissipation rate

Total energy dissipation rate is calculated by the following Eq. (2).

$$E_T = \sum E_{P,i} + \sum E_S + \sum E_F \quad (2)$$

where, $\sum E_{P,i}$ is the internal energy dissipation rate, $\sum E_S$ is the shear energy dissipation rate, $\sum E_F$ is the friction energy dissipation rate. They are calculated as follows :

$$E_{P,i} = \int_V \sigma \dot{\epsilon}_i dV, \quad E_S = \frac{\sigma_0}{\sqrt{3}} \int_S |\Delta V| dS,$$

$$E_F = \frac{m\sigma_0}{\sqrt{3}} \int_A |\Delta V| dA$$

3. Results and Discussions

Utilizing the formulated velocity, numerical calculations have been carried out to inspect the effect of process variables. An arc with radius M has been introduced to represent the shape of die profile. Numerical calculations have been done to

inspect the effect of process variables and calculated solutions are compared with the experimental results. Analyses were performed by using mechanical properties of Al 2218 aluminum alloy. The flow stress at room temperature was assumed to be independent of the strain rate and was modeled with the Ludwik-Hollomon equation :

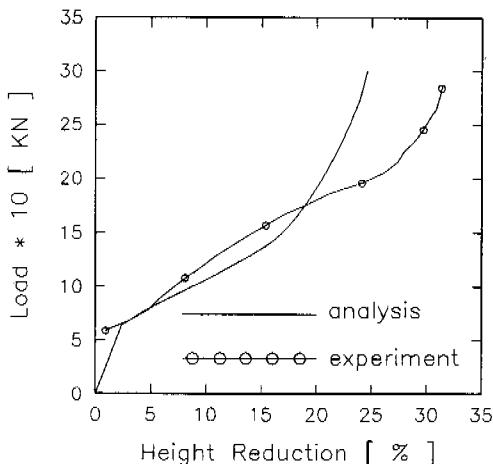
$$\bar{\sigma} = 352.48(\bar{\epsilon})^{0.2320} \text{ MPa}$$

The chemical composition of Al 2218 is shown in Table 1.

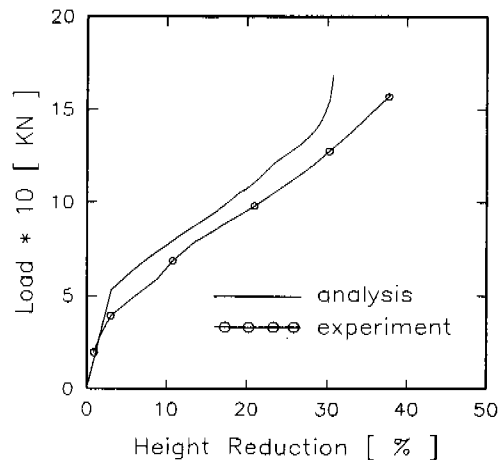
The calculated solutions and experimental inspections for forging of trochoidal gear with 12 teeth are plotted with respect to the height reduction as shown in Fig. 2. For hollow billet (Fig. 2 (b)), the calculated loads are in good agreement with the experimental results. This means that the solutions from the suggested velocity fields are useful to predict the final step load that is important to determine the capacity of forging equipment. As shown in the Fig. 2, for both hollow and solid billets, height reduction of the experiment

Table 1 Chemical compositions of wrought Al 2218.

Composition (%)							
Al	Si	Cu	Mn	Mg	Fe	Zn	Others
92.5	0.30	3.54	0.05	1.30	0.10	0.03	1.73Ni 0.01Cr



(a) Solid



(b) Hollow

Fig. 2 Relative pressures and loads for forging of trochoidal gear.

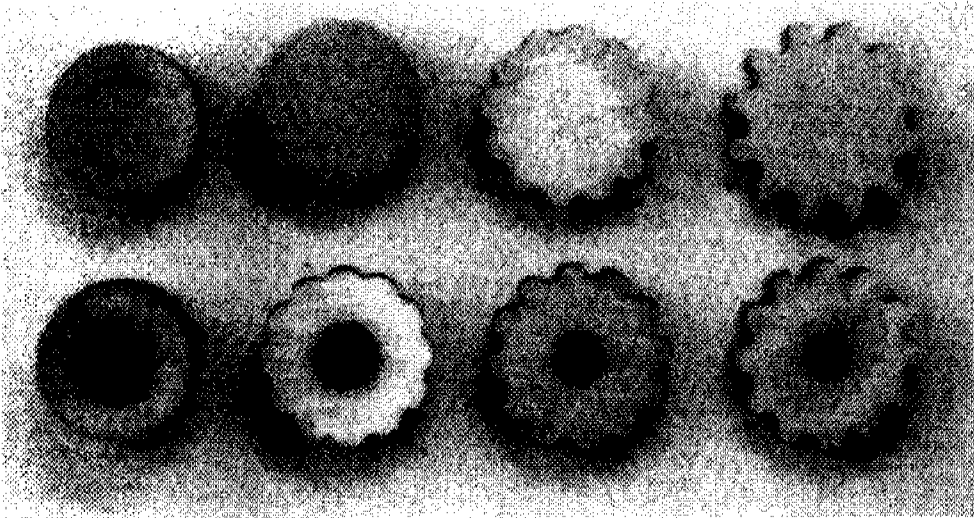


Fig. 3 Photographs of forged trochoidal gear for each step.

result is larger than that of the analysis. It should be caused by the following two reasons. One is elastic deformation of forging equipment and workpiece. The other is metal flow called as flash through the clearance between die-wall and a punch. Due to the backward extrusion, flash appears and grows in the axial direction with increasing height reduction. It is considered that the material flow is the main reason for the difference between an alysis and experiment in height reduction.

In the analysis by means of upper bound method for forging operation, the assumption of free flow surface profile is important to predict the forging load at the final step. In this study, it is assumed as a circle. Photographs of a forged trochoidal gear at each step are shown in Fig. 3. The free flow surface during the forging operation of a trochoidal gear is nearly a circle centered at O. So, it is considered that the assumption of free flow surface as a circle is in good agreement with that of experimental inspections. The dimensions of the billets used in the experiment are shown in Table 2.

The tooth profile for simulation is a quarter of a circle which is different from the actual one with half tooth height only up to a fillet or 2/3 tooth height up to a fillet and an arc(HJ in Fig. 1). Therefore, it is considered that the suggested

Table 2 Dimensions of billet and specification of gear used in forging experiment (unit : mm).

	billet			gear	
	Outer diameter	Inner diameter	Height	No. of teeth	Pitch circle diameter
Hollow	19.40	9.50	17.80	12	24.0
Solid	19.40	—	13.30	12	24.0

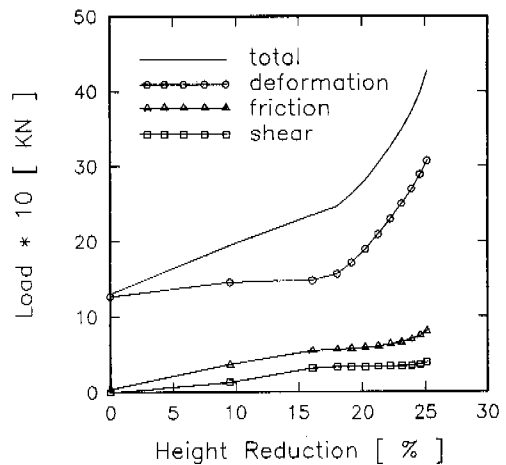


Fig. 4 Variations of energies with respect to reduction in height.

upper bound solutions can be applied to forging of trochoidal gear regardless of tooth height.

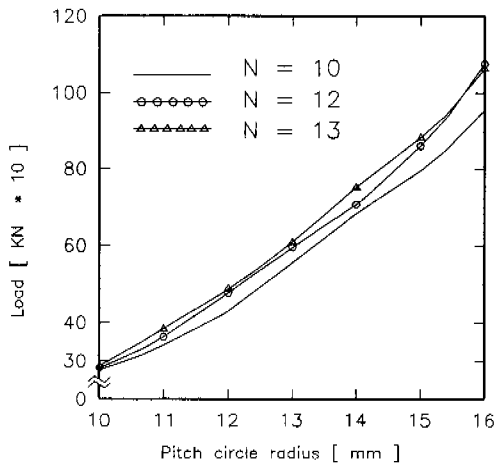
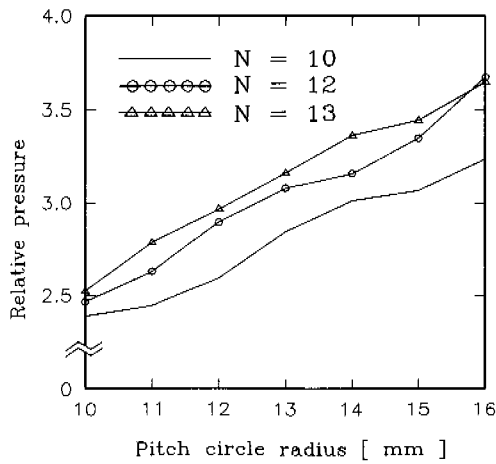


Fig. 5 Variations of loads and relative pressures in case of constant number of teeth.

Variations of energies—deformation, shear, friction—versus height reduction for forging of gear with number of teeth 12 are plotted in Fig. 4. Total energy was strongly affected by the deformation energy. The friction energy is higher than the shear energy. Therefore, it is considered that the actual material flow during forging of trochoidal gear is well represented by the division of deformation zone and the suggested velocity fields for the divided deformation zones.

Variations of loads and relative pressures are plotted with respect to the pitch circle radius in Fig. 5. As shown in the figure, the load and relative pressure increase as the pitch circle radius

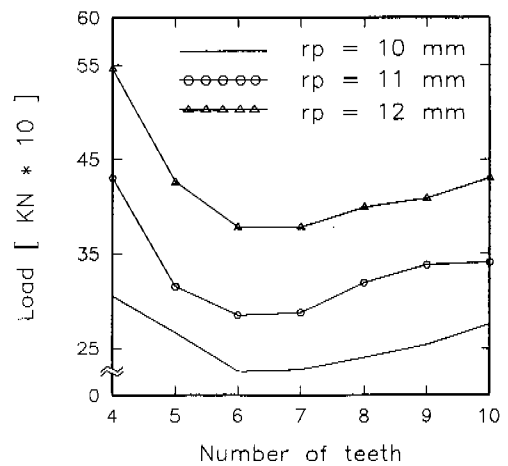
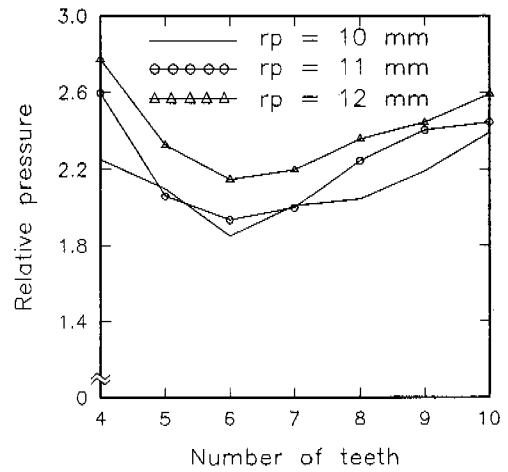


Fig. 6 Variations of loads and relative pressures in case of constant radius of pitch circle.

increases regardless of the number of teeth. Also, it appears that, for the same radius of a pitch circle, the load and relative pressure are dependent on the number of shear planes which exist in the deformation zones.

At the final step, forging load and relative pressure are shown in Fig. 6. We find that the load and relative pressure increase as in fig. 5 and find the minimum value for the given radius of pitch circle. In fig. 6, trochoidal gear with 6 or 7 teeth can be forged with the minimum value. Therefore, an optimal condition for forging of trochoidal gear can be found by the suggested kinematically admissible velocity field.

4. Conclusions

Forging of trochoidal gears has been investigated by means of upper-bound analysis and compared with experimental results using commercial aluminum alloy A/2218. The following conclusions can be drawn:

(1) A kinematically admissible velocity field for forging of trochoidal gears by using cylindrical billet has been newly proposed. Load requirements and optimal conditions for forging of trochoidal gears were successfully calculated by numerical method. It was found that the calculated solutions are in good agreement with the experimental results. Therefore, kinematically admissible velocity field of this study is very useful to predict the load requirement for forging of trochoidal gears.

(2) For forging of component with an arc shape tooth, the assumption of circular free flow surface is good to analyze the forging of trochoidal gear. The suggested velocity field is useful to predict the forging load.

(3) Load and relative pressure are dependent on the pitch circle radius for a given number of teeth. We can find the optimal condition with the minimum load and relative pressure for forging of trochoidal gear.

(4) The suggested velocity fields closely represent the actual material flow during forging of trochoidal gear.

Reference

- Cho, H. Y., 1991, "A Study on the Cold Extrusion of Helical Gear," Ph. D. Thesis, Pusan National University, (in Korean).
- Kim, D. K., 1996, Upper Bound Analysis of the Square Die Extrusion of Non-Axisymmetric Section," Ph. D. Thesis, Pusan National University, (in Korean).
- Grover, O. P. and Juneja, B. L., 1984, "Analysis of Closed-Die Forging of Gear-Like Elements," *Advanced Tech. of Plasticity*, 11, 888.
- Ohga, K., Kondo, K. and Jitsunari, T., 1985, "Research on precision Die Forging Utilizing Divided Flow," *Bulletin of the JSME*, 28, 2451.
- T. Jitsunari, K., Kondo, and Ohga, K. 1985, "Investigation on Cold Die Forging of a Gear Utilizing Divided Flow," *Bulletin of JSME*, 28, 2442.
- Abdul, N. A. and Dean, T. A., 1986, "An Analysis of the Forging of Spur Gear Forms," *Int. J. Mach. Tool Des. Res.*, 26, 113.
- Kiuchi, M. 1986, "Complex Simulation System of Forging Based on UBET," *Annals of the CIRP*, 35/1, 147.
- Kiuchi, M., Muramatsu, T. and Imai, T., 1989, "Analysis on Non-Axisymmetric Complex Forging," *J. of the JSTP*, 30, 997.
- Choi, J. C., Hur, K. D., Kim, C. H. Choi, J. U., 1994, "An Upper Bound Analysis for Closed-Die Forging of Spur Gear," *Forms, J. of KSPE*, 11, 26, (in Korean).
- Cho, H. Y., Choi, J. C., Choi, J. U. Min, G. S., 1995, "A Study on the Forging of Spur Gear with Variation of Inner Diameter in Hollow Billet," *J. of KSTP*, 4, 257, (in Korean).
- Cho, H. Y., Choi, J. U. Min, G. S., 1996, "Study on the Forging of Spline with Hollow and Solid Billets," *J. of KSPE*, 13, 108, (in Korean).